

1 **Palaeogenomic analysis of black rat (*Rattus rattus*) reveals multiple European introductions**
2 **associated with human economic history**

3

4 **Authors**

5 He Yu^{1,57}, Alexandra Jamieson^{2,55}, Ardern Hulme-Beaman^{3,4}, Chris J. Conroy⁵, Becky Knight⁶,
6 Camilla Speller^{7,8}, Hiba Al-Jarah⁷, Heidi Eager⁹, Alexandra Trinks^{2,10}, Gamini Adikari¹¹, Henriette
7 Baron¹², Beate Böhlendorf-Arslan¹³, Wijerathne Bohingamuwa¹⁴, Alison Crowther^{15,16}, Thomas
8 Cucchi¹⁷, Kinie Esser¹⁸, Jeffrey Fleisher¹⁹, Louisa Gidney²⁰, Elena Gladilina²¹, Pavel Gol'din²², Steven
9 M. Goodman²³, Sheila Hamilton-Dyer²⁴, Richard Helm²⁵, Chris Hillman²⁶, Nabil Kallala²⁷, Hanna
10 Kivikero²⁸, Zsófia E. Kovács²⁹, Günther Karl Kunst²⁰, René Kyselý³¹, Anna Linderholm³², Bouthéina
11 Maraoui-Telmini³³, Arturo Morales-Muñiz³⁴, Mariana Nabais^{35,36}, Terry O'Connor⁷, Tarek Oueslati³⁷,
12 Eréndira M. Quintana Morales³⁸, Kerstin Pasda³⁹, Jude Perera⁴⁰, Nimal Perera⁴⁰, Silvia Radbauer⁴¹,
13 Joan Ramon⁴², Eve Rannamäe⁴³, Joan Sanmartí Grego⁴⁴, Edward Treasure⁴⁵, Silvia Valenzuela-
14 Lamas⁴⁶, Inge van der Jagt⁴⁷, Wim Van Neer^{48,49}, Jean-Denis Vigne¹⁷, Thomas Walker⁵⁰, Stephanie
15 Wynne-Jones⁶, Jørn Zeiler⁵¹, Keith Dobney^{3,52,53,54}, Nicole Boivin^{15,16}, Jeremy B. Searle⁹, Ben Krause-
16 Kyora⁵⁵, Johannes Krause^{1,56,*}, Greger Larson^{2,*}, David Orton^{7,*}

17

18 ¹Department of Archaeogenetics, Max Planck Institute for the Science of Human History, Jena 07745,
19 Germany

20 ²Palaeogenomics & Bio-Archaeology Research Network, Research Laboratory for Archaeology and
21 History of Art, University of Oxford, Oxford OX1 3QY, United Kingdom

22 ³Department of Archaeology, Classics and Egyptology, University of Liverpool, Liverpool L69 7WZ,
23 United Kingdom

24 ⁴Research Centre in Evolutionary Anthropology and Palaeoecology, Liverpool John Moores
25 University, Liverpool L3 3AF, United Kingdom

26 ⁵Museum of Vertebrate Zoology, University of California, Berkeley, Berkeley, CA 94720-3160, USA

27 ⁶Department of Archaeology, University of York, York YO1 7EP, United Kingdom

28 ⁷BioArCh, Department of Archaeology, University of York, York YO1 7EP, United Kingdom

29 ⁸Department of Anthropology, University of British Columbia, Vancouver, BC, Canada

30 ⁹Department of Ecology and Evolutionary Biology, Cornell University, Ithaca, NY 14853, USA

31 ¹⁰Charité – Universitätsmedizin Berlin, Institut für Pathologie, Charitéplatz 1, 10117 Berlin,
32 Deutschland

33 ¹¹Postgraduate Institute of Archaeology, 407, Baudhaloka Mawatha, Colombo -7, Sri Lanka.

34 ¹²Römisch-Germanisches Zentralmuseum, Leibniz-Forschungsinstitut für Archäologie, Ernst -
35 Ludwig-Platz, 2D – 55116, Mainz, Germany

- 36 ¹³Christian Archaeology and Byzantine Art History, Philipps University of Marburg, 35037 Marburg,
37 Germany
- 38 ¹⁴Department of History and Archaeology, University of Ruhuna, Matara - 81000, Sri Lanka.
- 39 ¹⁵Department of Archaeology, Max Planck Institute for the Science of Human History, Jena 07745,
40 Germany
- 41 ¹⁶School of Social Science, The University of Queensland, St Lucia, Queensland, Australia.
- 42 ¹⁷Archaeozoology, Archaeobotany, Societies, Practices, Environments (AASPE-UMR7209), CNRS,
43 National Museum of Natural History (MNHN), Paris, France
- 44 ¹⁸Archeoplan Eco, 2616 LZ, Delft, Netherlands
- 45 ¹⁹Department of Anthropology, Rice University, 6100 Main St, Houston, TX 77005
- 46 ²⁰Archaeological Services, University of Durham, United Kingdom
- 47 ²¹Ukrainian Scientific Centre of Ecology of the Sea, Odessa 65009, Ukraine
- 48 ²²Schmalhausen Institute of Zoology, National Academy of Sciences of Ukraine, Kiev 01030, Ukraine
- 49 ²³Negaunee Integrative Research Center, Field Museum of Natural History, Chicago, IL 60605, USA
- 50 ²⁴Department of Archaeology & Anthropology, Bournemouth University (Visiting Fellow), Poole,
51 BH12 5BB, United Kingdom
- 52 ²⁵Canterbury Archaeological Trust, 92a Broad Street, Canterbury, Kent CT1 2LU, UK
- 53 ²⁶6 Fell View Park, Gosforth, Seascale, Cumbria, CA20 1HY, UK
- 54 ²⁷Institut National du Patrimoine, Tunis 1008, Tunisia
- 55 ²⁸University of Helsinki, Department of Culture, P.O. Box 59, FI-00014 Helsinki, Finland
- 56 ²⁹Freelance archaeozoologist, Liliom u. 4. 1/1., Balatonfüred, 8230, Hungary
- 57 ³⁰VIAS Vienna Institute for Archaeological Science, University of Vienna, Althanstraße 14, 1090
58 Vienna, Austria
- 59 ³¹Department of Natural Sciences and Archaeometry, Institute of Archaeology of the Czech Academy
60 of Sciences, Prague, Letenská 4, 118 01, Prague, Czech Republic
- 61 ³²Department of Anthropology, Texas A&M University, College Station, TX 77843, USA
- 62 ³³Department of History, University of Tunis, Tunis, Tunisia
- 63 ³⁴Departamento de Biología, Universidad Autónoma de Madrid, 28049 Madrid, Spain
- 64 ³⁵Institute of Archaeology, University College London, London WC1H 0PY, UK
- 65 ³⁶Centro de Arqueologia da Universidade de Lisboa (UNIARQ), Faculdade de Letras, Universidade
66 de Lisboa, 1600-214 Lisboa, Portugal
- 67 ³⁷Centre National de la Recherche Scientifique, University of Lille, France
- 68 ³⁸Department of Anthropology, University of California, Santa Cruz, 1156 High St, Santa Cruz, CA
69 95064, USA
- 70 ³⁹Department of Philosophy, Institute of Prehistoric Archaeology, Friedrich-Alexander-University of
71 Erlangen-Nürnberg, 91054 Erlangen, Germany
- 72 ⁴⁰Department of Archaeology, Sir Marcus Fernando Mawatha, Colombo-07, Sri Lanka

- 73 ⁴¹Austrian Academy of Sciences, Austrian Archaeological Institute, Hollandstraße 11-13, 1020
74 Vienna, Austria
- 75 ⁴²Consell Insular d'Eivissa i Formentera
- 76 ⁴³Department of Archaeology, Institute of History and Archaeology, University of Tartu, 2 Jakobi St.,
77 51005 Tartu, Estonia
- 78 ⁴⁴Secció de Prehistòria i Arqueologia, University of Barcelona, Spain
- 79 ⁴⁵Department of Archaeology, Durham University, Durham, UK
- 80 ⁴⁶Archaeology of Social Dynamics, IMF-CSIC, Barcelona 08001, Spain
- 81 ⁴⁷Cultural Heritage Agency of the Netherlands, Smallepad 5, 3811 MG Amersfoort, The Netherlands
- 82 ⁴⁸Royal Belgian Institute of Natural Sciences, Vautierstraat 29, 1000 Brussels, Belgium
- 83 ⁴⁹Laboratory of Biodiversity and Evolutionary Genomics, Katholieke Universiteit Leuven, 3000 Leuven,
84 Belgium
- 85 ⁵⁰Department of Archaeology, University of Reading, Berkshire RG6 6AB, United Kingdom
- 86 ⁵¹ArchaeoBone, 9753 JN Haren, The Netherlands
- 87 ⁵²Department of Archaeology, University of Sydney, Sydney, Australia
- 88 ⁵³Department of Archaeology, University of Aberdeen, Aberdeen, UK
- 89 ⁵⁴Department of Archaeology, Simon Fraser University, Burnaby, Canada
- 90 ⁵⁵Institute of Clinical Molecular Biology, Kiel University, Kiel 24105, Germany
- 91 ⁵⁶Max Planck Institute for Evolutionary Anthropology, Leipzig 04103, Germany

92

93 ⁵⁷These authors contributed equally

94 *Correspondence: krause@eva.mpg.de, greger.larson@arch.ox.ac.uk, david.orton@york.ac.uk

95

96 **Abstract**

97 The distribution of the black rat (*Rattus rattus*) has been heavily influenced by its association with
98 humans. The dispersal history of this non-native commensal rodent across Europe, however, remains
99 poorly understood, and different introductions may have occurred during the Roman and medieval
100 periods. Here, in order to reconstruct the population history of European black rats, we generated a *de*
101 *novo* genome assembly of the black rat, 67 ancient black rat mitogenomes and 36 ancient nuclear
102 genomes from sites spanning the 1st-17th centuries CE in Europe and North Africa. Analyses of
103 mitochondrial DNA confirm that black rats were introduced into the Mediterranean and Europe from
104 Southwest Asia. Genomic analyses of the ancient rats reveal a population turnover in temperate
105 Europe between the 6th and 10th centuries CE, coincident with an archaeologically attested decline in
106 the black rat population. The near disappearance and re-emergence of black rats in Europe may have
107 been the result of the breakdown of the Roman Empire, the First Plague Pandemic, and/or post-
108 Roman climatic cooling.

109

110 **Introduction**

111 The black rat (*Rattus rattus*) is one of three rodent species, along with the house mouse (*Mus*
112 *musculus*) and brown rat (*Rattus norvegicus*), to have become globally distributed thanks to a close
113 commensal relationship with humans¹. Collectively, these taxa are highly significant to human
114 societies both as pests responsible for billions of euros of damage to food stores annually², and as
115 vectors and/or reservoirs that have contributed to the spread of numerous diseases, most infamously
116 bubonic plague^{3,4}.

117

118 Despite the significance of this rodent, our knowledge of the black rat's evolutionary history and
119 taxonomy remains limited. Previous genetic studies have described a *R. rattus* complex involving
120 multiple recognized species with potential introgression among different lineages⁵⁻⁷. Mitochondrial
121 DNA studies have helped to resolve the taxonomic controversies by linking a monophyletic
122 mitochondrial lineage to specific South Asian (now globally distributed) *R. rattus* populations that
123 possess a 2n=38 karyotype (previously referred to as lineage I)⁸⁻¹⁰. The Asian house rat (*Rattus*
124 *tanezumi*), endemic to Southeast Asia, has been identified as the closest sister group of the black rat
125 (previously designated as lineages II through IV). The divergence between the two species has been
126 dated to ~0.4 Mya¹¹, and the two have been suggested to hybridise^{6,7,12}.

127

128 The ability of rats to colonise, and become dependent upon, anthropogenic niches¹³ makes them ideal
129 bioproxies to track historical processes^{1,14,15}. Archaeological specimens of rats and mice have thus
130 been used to track human migrations, trade, and settlement types in a wide range of contexts¹⁶⁻²².
131 Previous archaeological and genetic evidence suggests that the pre-commensal distribution of the
132 Eurasian black rat (based on the taxonomic definition proposed by mitochondrial DNA studies^{8,9} and
133 hereafter referred to as black rat, see SI for discussion) was largely limited to South Asia^{10,23,24}. Black
134 rat finds from cave sediments in the Levant spanning the late Pleistocene to early Holocene indicate a
135 possible western distribution^{25,26}. These remains require direct dating to confirm their age, and there
136 is a subsequent absence of rats from settlement sites in this region until at least the 2nd millennium
137 BCE²⁶.

138

139 The earliest large concentrations of presumed commensal rat remains reported thus far derive from
140 late third, or early second millennium BCE settlements in both the Indus Valley and Mesopotamia²⁶.
141 Commensal black rats may also have reached the Levant and eastern Mediterranean region by the
142 start of the first millennium BCE²⁶. Based on archaeological evidence from Corsica, the Balearics,
143 Italy and Morocco²⁷⁻²⁹, black rats likely first appeared in the western Mediterranean basin towards the
144 end of that same millennium.

145

146 The colonisation of Europe by the black rat has been linked to the historical development of urbanism
147 and trade networks, and their arrival is important for understanding historical plague pandemics
148 including the 6th C Justinianic Plague and the 14th C Black Death ^{4,30-32}. The central role traditionally
149 attributed to black rats and their fleas in the spread of the plague bacterium (*Yersinia pestis*) during
150 these pandemics has been challenged on various grounds, however, including the historical
151 distribution and abundance of rats, and this correlation continues to be debated ³³⁻³⁷.

152

153 Although surveys of zooarchaeological rat finds from archaeological sites across Europe suffer from
154 considerable regional variation in coverage, the available data indicates successive episodes of
155 dispersal north of the Mediterranean associated first with Roman expansion (first century BCE to
156 second century CE), and then with the emergence of medieval economies from the 9th century CE,
157 punctuated by a decline and possible range contraction ³². Black rat remains are found throughout the
158 Roman Empire in the 1st to 5th centuries CE, but rarely beyond its northern borders suggesting that
159 these rats were dependent on a Roman economic system characterised by a network of dense
160 settlements connected by bulk transport via efficient road, river, and maritime routes ^{4,31}.

161

162 With the breakdown of the Roman Empire from the 5th century onwards, evidence for the existence of
163 black rats becomes scarcer. They may have been extirpated entirely from the northern provinces
164 including Britain ^{32,38,39}, and the percentage of archaeological sites with black rat remains declined
165 even in the Western Empire's Italian core ⁴⁰. By contrast, black rats remained common in the Balkans
166 and Anatolia until at least the 6th century CE, presumably reflecting continued stability in the Eastern
167 Roman Empire ⁴¹⁻⁴⁴. Since 5th-8th century zooarchaeological data is limited in many regions, the
168 pattern of post-Roman absence may partly represent research bias ⁴⁵, though early medieval black rats
169 are rare even where other small mammals are reported ³⁸.

170

171 Black rats reappear at northern European trading settlements during the 9th and 10th centuries CE,
172 including sites well beyond their Roman range, including Hedeby in northern Germany and Birka in
173 Sweden, as well as former Roman towns and high-status early medieval settlements such as York and
174 Flixborough in England and Sulzbach in Bavaria ⁴⁶⁻⁵⁰. The subsequent expansion of urbanism and
175 large-scale trade of bulk goods in medieval Europe appears to have favoured rats, just as in the
176 Roman period. By the 13th century CE, black rats were present throughout most of Europe ⁴ and they
177 reached southern Finland by the late 14th century ⁵¹. Rats remained widespread across Europe until at
178 least the 18th century, before their population declined, most likely as a result of competition with the
179 newly arrived brown rat, the now dominant rat species in temperate Europe ⁵²⁻⁵⁴.

180

181 It remains unclear whether the black rat was actually extirpated from post-Roman northern and
182 western Europe; and whether medieval rat populations in temperate Europe derived from the remnant

183 population in southern Europe, or from another wave of rats that were introduced from beyond the
184 Mediterranean (e.g. via Rus' river trade ^{32,55}). These questions are relevant to several key debates in
185 European economic and environmental history including: 1) the extent to which the end of the
186 Western Roman Empire represented a crisis in urbanism and trade — particularly in bulk goods such
187 as grain — as well as political collapse ^{56–58}; 2) the role of easterly vs. westerly connections in the rise
188 of northern European medieval urban networks ^{59,60}; and 3) the model of the spread of the Justinianic
189 Plague and the subsequent First Pandemic. This pandemic started in the eastern Mediterranean in 541
190 CE, spread quickly across Europe and England, and continued for approximately two centuries ^{61–63}, a
191 period that coincides with the gap in archaeological evidence for rats in northwest Europe. Given the
192 limitations of both zooarchaeology and genetic studies of modern rat populations to address
193 successive waves of contact after a species is established, ancient DNA may help to resolve these
194 questions by directly revealing the presence or lack of genetic continuity through time.

195

196 We employed a nested three-stage approach to address these questions. First, we assembled a *de novo*
197 reference genome of the black rat. This genome allowed us to investigate the long-term demographic
198 history of *Rattus rattus* in relation to other rat species, and to lay the foundation for genome-wide
199 analyses of ancient remains. Second, we explored the dispersal of black rats into the Mediterranean
200 and Europe by analysing 70 new mitochondrial genomes from European and North African
201 archaeological specimens spanning the Roman to early post-medieval periods (1st-17th century CE),
202 alongside 132 mtDNA sequences generated from modern and museum black rat specimens from
203 across western Eurasia, the Indian Ocean, and Africa. Lastly, we generated 39 nuclear genomes from
204 our archaeological black rats and used these to explore the species' population history in Europe and
205 the Mediterranean from the 1st to 17th centuries CE, focusing particularly on the hypothesis of dual
206 dispersals in the Roman and medieval periods. We then interpreted the black rat's dispersal history
207 within the context of major historical processes.

208

209 **Results and Discussion**

210 **The demographic history of *Rattus rattus* and its closely related species**

211 To facilitate the study of the demographic history of the black rat, both before and after the
212 establishment of its commensal relationship with humans, we first generated a *de novo* genome
213 assembly of *R. rattus* using a wild-caught black rat from California, USA. Combining shotgun,
214 Chicago and Hi-C sequencing data with the Dovetail HiRise assembler pipeline ⁶⁴, we obtained a
215 genome assembly with a total length of 2.25 Gb and a scaffold N50 reaching 145.8 Mb
216 (Supplementary Table 1, 2). The 22 scaffolds with over 10 Mb covering 98.9% of the entire assembly
217 (Table 1), with each of the 18 autosomes of *R. rattus* corresponding to one large scaffold each and
218 over 90% of the X chromosome represented by four scaffolds (Supplementary Figure 11, 12, Note 2).
219 The average GC content is 42.1%, similar to the *R. norvegicus* reference genome *Rnor_6.0* (42.3%),

220 and 38.4% of the assembly was identified as repetitive elements (Supplementary Table 3).
221 Benchmarking Universal Single-Copy Orthologs (BUSCO) analysis ⁶⁵ also revealed a high
222 completeness of this genome assembly, with 90.1% complete BUSCOs identified using eukaryotic
223 dataset, comparable with *Rnor_6.0* (91.4%) (Supplementary Table 4). Because *R. tanezumi* and *R.*
224 *rattus* are both present in California, we also assessed potential introgression from *R. tanezumi* into
225 our *R. rattus* individual. A signature of introgression would limit the value of our *de novo* genome as
226 a reference genome onto which reads derived from ancient black rats could be mapped. Our analyses
227 suggested no significant introgression signature in the Californian black rat (Supplementary Note 5).

228

229

Table 1. Assembly statistics of the *de novo* *R. rattus* reference genome

Scaffold Number	6805
Scaffold N50 (Mb)	145.8
Largest Scaffold (Mb)	260.8
Assembly size (Gb)	2.25
Scaffold length >10 Mb (Gb)	2.23
GC content (%)	42.1
Repetitive region (%)	38.4

230

231 To address the demographic history of black rat, we applied the Pairwise Sequentially
232 Markovian Coalescent (PSMC) ⁶⁶ analysis to estimate its population size dynamics alongside the
233 brown rat and Asian house rat. When calibrated with a mutation rate of 2.96×10^{-9} per generation and
234 generation time of 0.5 years ⁶⁷, the analyses revealed different dynamic patterns of population size
235 changes amongst these rat species (Figure 1A). The brown rat experienced a population decline
236 beginning ~1 Mya, as described previously ⁶⁷, while both the black rat and Asian house rat
237 populations expanded until 300-400 thousand years ago (kya). The black rat population then
238 experienced a bottleneck with an 8-fold drop in effective population size until 100 kya, and a re-
239 expansion from 100 kya to 40 kya. The Asian house rat, however, did not experience a population
240 decline until ~40 kya, when both black rat and Asian house rat populations experienced declines that
241 have continued to the present.

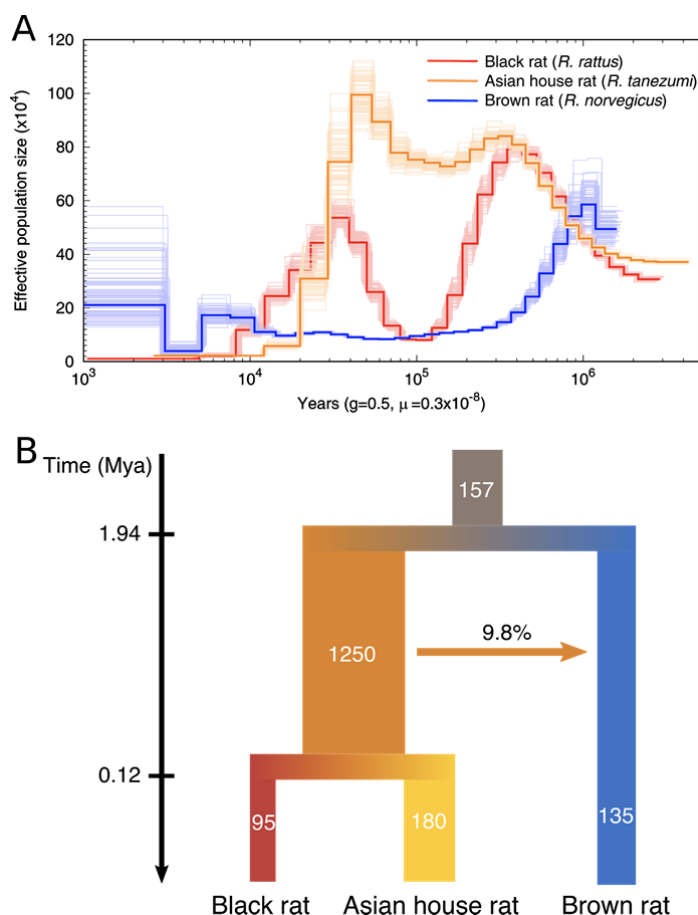
242

243 To investigate the population sizes, split times, and migrations among these rat lineages, we applied
244 Generalized Phylogenetic Coalescent Sampler (G-PhoCS) ⁶⁸. The result revealed a similar population
245 size dynamism, with the effective population size (N_e) of black rat/Asian house rat ancestral lineage
246 estimated to be 1.25×10^6 , about tenfold the N_e of black rat/Asian house rat/brown rat lineages (Figure
247 1B, Supplementary Table 5, 6). The split time between brown rat and black rat/Asian house rat
248 lineages was estimated to be 1.94 Mya (within the 95% Highest Posterior Density (HPD) range
249 estimated using mitochondrial genomes in a previous study ¹¹), while the split of Asian house rat and

250 black rat lineages took place ~120 kya. This recent split time relative to the coalescent time estimate
251 based on mitochondrial genomes between these two lineages could be explained by the large ancestral
252 population size of the black rat/Asian house rat lineage⁶⁸. Among these lineages, we only detected
253 one instance of gene flow from the black rat/Asian house rat ancestral lineage into brown rat lineage,
254 with an introgression proportion of 9.8%.

255

256 Taken together, we observed population expansions and bottlenecks in the black rat during the last
257 million years, and a smaller N_e relative to the Asian house rat. This could be explained by the
258 relatively limited geographic distribution of the black rat in southern Asia before the initiation of its
259 commensal relationship with people, and the fact that the Asian house rat is endemic to a much
260 greater area in southeastern Asia¹⁰. We did not detect any genomic introgression between the lineages
261 leading to the black and Asian house rat, suggesting these two species were geographically isolated
262 after their split from a common ancestor for a sufficiently long period to facilitate their reproductive
263 incompatibility.



264

265 **Figure 1. The demographic history of the black rat and its closely related species.**

266 (A) Population dynamics of the black rat (*R. rattus*), Asian house rat (*R. tanezumi*) and brown rat (*R.*
267 *norvegicus*) estimated by PSMC, with 100 bootstrap replicates.

268 **(B)** Demographic modelling of the divergence and migration among the black rat, Asian house rat and
269 brown rat estimated by G-PhoCS. The values represent the average estimates of effective population
270 sizes (in thousands), population divergence times (Mya) and the total migration rate through time. The
271 95% HPD range of all estimates are listed in Supplementary Table 6.

272

273 **A global phylogeography of the black rat based on mitochondrial DNA**

274 We collected 191 ancient black rat individuals from 33 archaeological sites across Europe, North and
275 East Africa, and southern Asia dating from the 2nd millennium BCE to the 17th century CE
276 (Supplementary Table 7), plus eight modern individuals from North Africa. After shotgun screening,
277 we retrieved 70 mitochondrial genomes (with coverage spanning 3.5x-300.0x) from samples from 18
278 sites in Europe and the Mediterranean (Supplementary Table 8), and identified 40 haplotypes. The
279 phylogenetic tree based on mitochondrial genomes revealed two clades: a major clade with 32
280 haplotypes, and a minor clade consisting of eight haplotypes and 23 ancient samples from the 6th-
281 century site of Caričin Grad, Serbia (Supplementary Figure 3). The phylogenetic resolution within
282 each major clade was relatively poor, though samples from the same or closely related sites
283 occasionally formed sub-clades including the samples from modern-day Zembra (Tunisia) and
284 medieval central Europe.

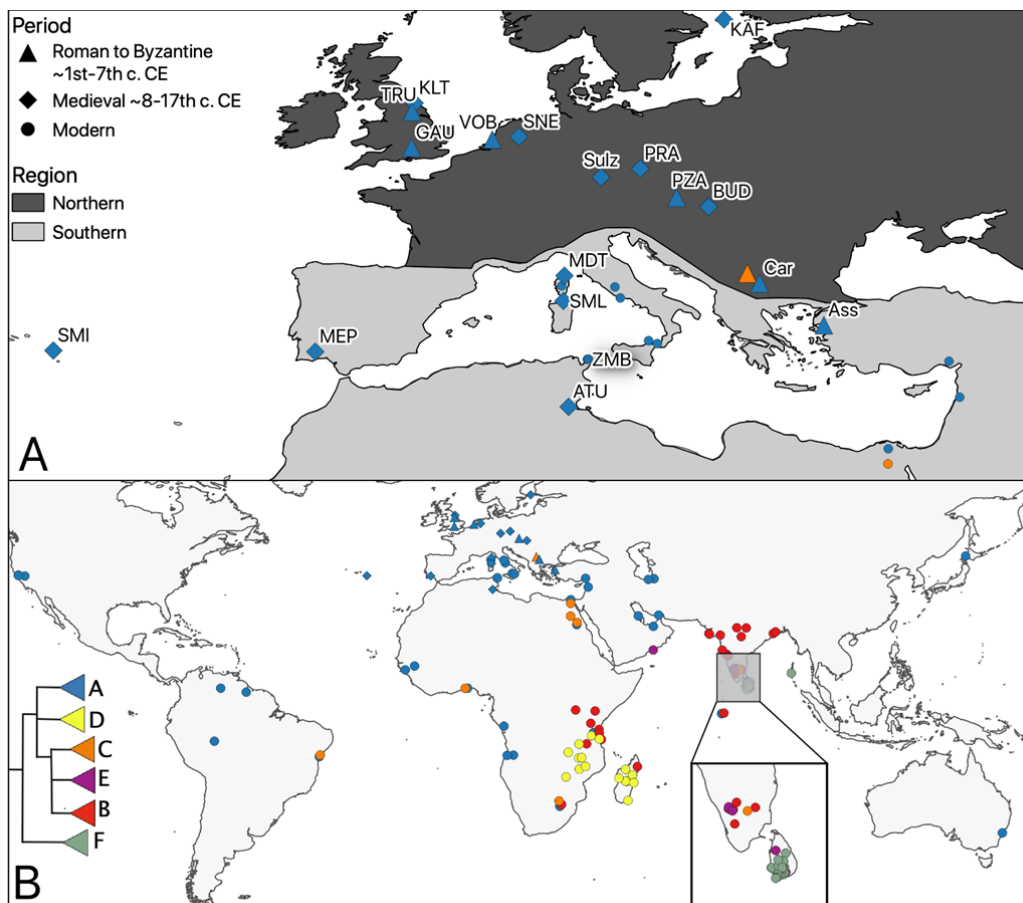
285

286 In order to establish the relationship between the ancient rats and modern black rats from across their
287 range, we analysed the cytochrome b (CYTB) region from our ancient samples alongside 132
288 previously unpublished modern CYTB sequences from across the Indian Ocean basin (Supplementary
289 Table 9), and sequences published in previous studies^{10,24,69,70}. The maximum likelihood tree of the
290 CYTB region revealed that all the ancient rats from this study belong to the previously described
291 black rat lineage I (Figure 2, Supplementary Figure 4, 5 and Table 10). None of the ancient rats from
292 this study fell into *Rattus* lineages II-VI. Within lineage I, we recapitulated the unnamed substructure
293 and assigned the terms A to E to the five major haplogroups¹⁰. In addition to these five, we confirmed
294 a sixth lineage I haplogroup, F, consisting of modern samples from Sri Lanka and the Andaman
295 Islands, which is basal relative to all other lineage I black rats and has previously been reported as the
296 Sri Lankan unique sub-lineage, RrC LIb⁷¹ (Figure 2, Supplementary Figure 4b, Table 10).

297

298 Haplogroup A within lineage I (previously described as the European ship rat²⁴) was the most
299 common among the analysed samples (179/354). Members of this haplogroup include ancient and
300 modern black rats from Europe and regions of the world with a history of colonisation by, and/or
301 trade with European powers. The only additional haplogroup found in Europe was Haplogroup C
302 (previously described as the Arab ship rat²⁴) at Caričin Grad, Serbia, which included 24
303 archaeological individuals. Haplogroup C is found in modern rats from India, Egypt, East, South and
304 West Africa and South America. None of the other haplogroups were present in Europe or the

305 Mediterranean region. Haplogroups B and E only included modern samples from India and countries
306 bordering the Indian Ocean. Haplogroup D (previously described as the Madagascar and Indian Ocean
307 islands group²⁴) included primarily samples from Madagascar and East Africa, and Haplogroup F
308 consisted of samples from Sri Lanka and the Andaman Islands (Figure 2, Supplementary Table 10).
309



310
311 **Figure 2. Sampling sites and mitochondrial phylogeographic patterns.**
312 A - Map of sampling locations. The ancient sample SMI only has mitochondrial data, the rest have
313 both nuclear and mitochondrial results. SMI (Villa Franca de Campo) MEP (Mertola) KLT (Kilron
314 Castle) TRU (Tanner Row, York) GAU (Gatehampton Villa) VOB (Voorburg-Forum Hadriani) SNE
315 (Deventer-Stadhuiskwartier) MDT (Monte di Tuda) SML (Santa Maria Lavezzi) ATU (Althiburos)
316 Sulz (Castle Sulzbach) PRA (Prague Castle) PZA (Petronell-Carnuntum Zivilstadt) KAF
317 (Kastelholm) BUD (Buda Castle-Teleki Palace) Car (Caričin Grad) Ass (Assos). B - The
318 phylogeographic pattern of black rat revealed by CYTB mitochondrial haplogroups (see
319 Supplementary Figure 4 for detailed phylogeny). We derived modern nuclear genomes from the
320 reference genome rat from California and individuals trapped on the island of Zembra (ZMB) in the
321 1980s that were prepared for a zooarchaeological reference collection.

322

323 To investigate the introduction route of black rats into Europe, we analyzed mitochondrial
324 cytochrome B sequences derived from globally distributed modern and ancient black rats. Previous
325 studies indicated that the black rat originated in the Indian Peninsula^{10,24,69,72}. Leaving aside the
326 putative late Pleistocene to early Holocene records from the eastern Levant, the earliest finds of
327 presumed commensal rats derive from the Indus Valley and Mesopotamia in the 3rd/2nd millennium
328 BCE, coincident with the emergence of urbanism and establishment of trade links between these
329 regions^{26,73}, though a more westerly limit to the black rat's natal range cannot be excluded. The
330 source for dispersal to the Mediterranean and ultimately Europe remains unclear. Suggestions include
331 maritime trade from India and/or the Arabian peninsula into the Red Sea and subsequently through
332 Egypt (perhaps via the canal built under Darius⁷⁴) in the mid/late first-millennium BCE^{4,32}, or more
333 likely earlier overland communication routes between Mesopotamia and the Levant^{26,73}.

334

335 While a maritime route is clearly implicated in the black rat's dispersal to East Africa^{75,76}, our results
336 tentatively favour an overland hypothesis for its dispersal from South Asia to the Mediterranean to
337 Europe, since both ancient and modern black rats from Europe and the eastern Mediterranean share
338 haplogroups with sampled populations from Iran and the Persian Gulf, but not with Indian Ocean
339 samples from southern India to Madagascar (Figure 2). The results also suggest a secondary dispersal
340 route via Egypt, given the appearance of Haplogroup C at the 6th century CE Byzantine site of Caričin
341 Grad, Serbia and in modern samples from the Nile valley. While tentative, this may reflect Egypt's
342 central roles both in direct Indo-Roman trade, following its annexation in 30 BCE, and in grain
343 production for the Roman and early Byzantine Empires^{4,77}. To test these hypotheses, further
344 investigations into ancient and modern black rat populations from the Levant, Mesopotamia, Egypt
345 and the Indus Valley are necessary.

346

347 **Ancient genomes reveal the relationships of European black rats over space and time**

348 To explore the black rat's European population history in greater detail, we shotgun sequenced 36
349 ancient and 3 modern black rats from 17 sites to 0.2x-16x coverage for whole genome analysis,
350 including 18 females and 21 males determined by the coverage on sex chromosomes (Supplementary
351 Table 11). The deeper sequenced ancient samples spanned two broad time periods, including 15 from
352 the Roman and Early Byzantine period (1st to 7th century CE), and 21 from medieval and post-
353 medieval contexts (8th to 17th century CE) (Supplementary Table 12). Geographically, all the samples
354 were divided into two groups: a "northern" group of 25 samples from temperate Europe, and a
355 "southern" group of 11 samples from the Mediterranean and Portugal (Figure 2). After mapping and
356 genotyping, we identified 7,869,069 bi-allelic transversion variants in the autosomal non-repetitive
357 regions for downstream population genetic analysis.

358

359 The phylogenetic tree constructed from autosomal SNPs revealed complex relationships among
360 ancient black rats from different regions and time periods (Figure 3A). Except for the late medieval (c.
361 14th century) to Ottoman (c. 17th century) site of Buda Castle, Hungary, samples from the same site
362 are clustered together. All the samples from the northern group, together with one southern sample
363 from the medieval period — from 8th-9th century Althiburos, Tunisia — formed a single clade, while
364 all the other Byzantine to medieval samples from the southern group formed several separate clades
365 consistent with their local geographic region. The rats from the southern group also possessed higher
366 heterozygosity than those from the northern group, within both Roman/Byzantine and medieval/post-
367 medieval periods (Supplementary Figure 7, Table 13). This could be explained by the longer history
368 of rats in the Mediterranean which date to at least the first millennium BCE^{26,27}, and the founder
369 effects of limited introductory waves of rats into the northern region.

370

371 Within the major northern cluster, samples were divided into two smaller clusters representing Roman
372 / Byzantine and medieval / post-medieval periods respectively. The only exception was a medieval
373 Tunisian sample that falls into the Roman cluster. Within each cluster, samples grouped together
374 based upon their geographic location (central Europe, western/northern Europe, Serbia). These
375 phylogenetic relationships suggest that the initial black rat population in temperate Europe was
376 replaced by a genetically distinct population after the 6th century CE. The later population is first
377 documented in early medieval (8th to early 10th century CE) Sulzbach, Germany. The Roman-like
378 gene pool was still present during the 8th-9th century in North Africa, though due to the lack of more
379 recent samples we cannot address whether or when the second wave arrived there. A similar pattern
380 was also revealed by multidimensional scaling (MDS) based on isolation-by-state (IBS) distance
381 among the samples (Supplementary Figure 8).

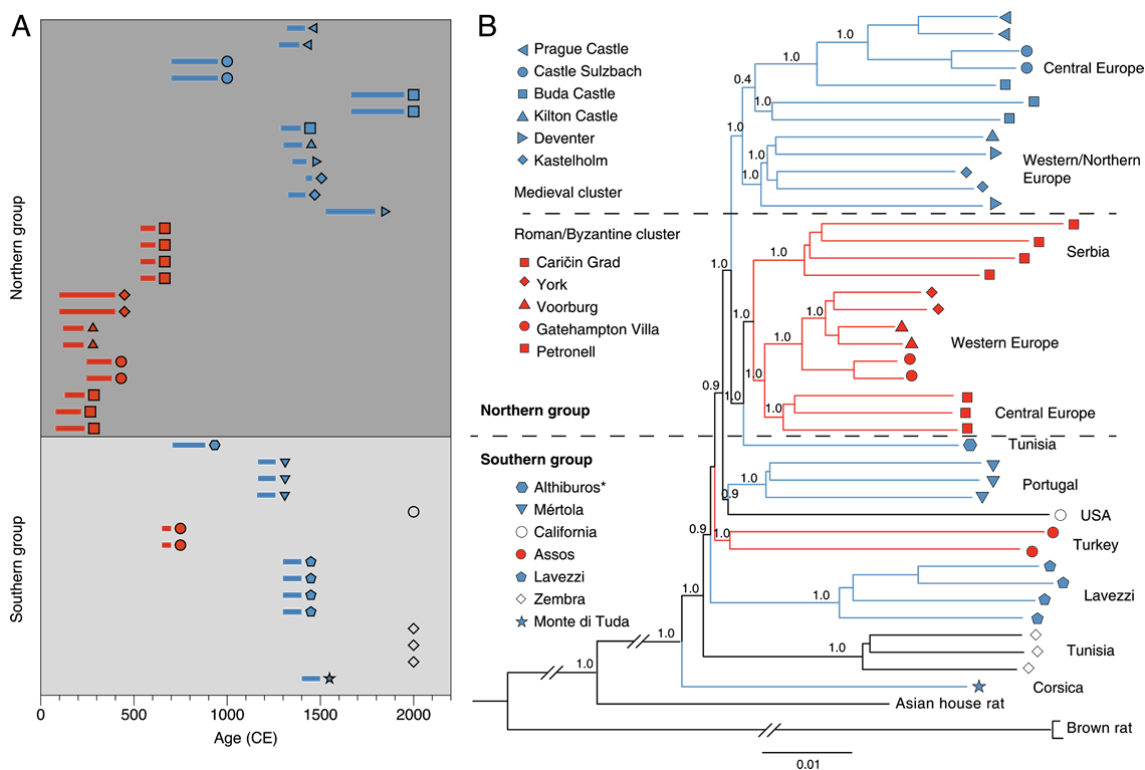
382

383 The phylogenetic tree based on Y-chromosome scpMSY regions (Supplementary Table 14) similarly
384 demonstrated that the Roman rats formed a single cluster. However, unlike the autosomal phylogeny,
385 all the post-Roman samples from both the northern and southern groups, including Byzantine Assos
386 and Caričin grad, formed a separate cluster (Supplementary Figure 9), without well-supported
387 substructures. Given the male-biased dispersal pattern commonly described in the black rat and other
388 rodent species^{78,79}, this might indicate a male-specific replacement that took place in both the
389 Mediterranean regions and temperate Europe.

390

391 A decline in the European black rat population during the 6th to 9th centuries has previously been
392 suggested based on zooarchaeological evidence^{32,38,39}. This has been attributed to several causes
393 including: (a) the demise of the Western Roman Empire's economic and urban system from the 5th
394 century CE, including the cessation of large-scale grain shipments that may have helped to disperse
395 and support rat populations⁴; (b) climatic cooling in the 'Late Antique Little Ice Age'⁸⁰; and/or (c)

396 the Justinianic Plague, which began in 541 CE and is likely to have infected rat populations
 397 previously naive to *Yersinia pestis*, regardless of their potential role in its spread among humans^{4,81,82}.
 398 Our finding of a post-6th-century turnover corroborates this apparent decline, though the density of our
 399 samples' spatiotemporal coverage is not sufficient for us to distinguish between the potential causes.
 400 To understand how the Justinianic Plague influenced the rat population, further studies should focus
 401 on archaeological black rats from contexts post-dating the mid-6th century in areas of the Byzantine
 402 Empire and wider Mediterranean where an urban settlement system persisted.
 403
 404 The medieval Tunisian (Althiburos) sample indicates a different population history of black rats in
 405 North Africa relative to temperate Europe. Black rats from a wider range of time periods resident in
 406 North Africa and the western Mediterranean would allow us to test whether there was continuity
 407 within the black rat populations from the Roman to early Islamic period (c.8th century). This is
 408 particularly pertinent to debates concerning the degree of continuity between the Roman Empire and
 409 the Early Islamic world, notably in urban settlements and trade networks⁸³.
 410



411
 412 **Figure 3. Relationships of the ancient black rats over time and space.**
 413 (A) The ages of the rat samples included in whole genome analyses. The bars represent 95.4%
 414 confidence intervals surrounding the direct radiocarbon dates or stratigraphic dates (Supplementary
 415 Table 11,12). The colors correspond to the Roman/Byzantine (red) and medieval (blue) time periods.

416 The symbols represent the sampling sites listed in panel B, and the modern samples are represented by
417 black symbols.

418 **(B)** The phylogenetic relationship among ancient and modern black rats reconstructed using a
419 neighbor joining phylogeny. The pairwise genetic distances were calculated using autosomal variants.
420 The support values based upon 100 bootstrap replicates are shown on the nodes. The branches are
421 colored by sample ages as described in panel A, and the tip symbols correspond to the sampling site.
422 * Though the medieval Tunisian (Althiburos) sample clusters geographically in the Southern group, it
423 falls in with the Roman cluster of the northern group in the phylogeny.

424

425 To investigate the genetic interaction between different rat populations further, we applied a series of
426 f_4 -statistics. Based on the result of the f_4 -statistics symmetry test, the ancient samples were divided into
427 18 groups (Supplementary Table 15). Sixteen of these correspond to samples from 16 different sites,
428 while the three late/post-medieval samples from Buda Castle (Hungary) fell into two groups
429 corresponding respectively to late medieval (14th-15th century) and Ottoman (17th century) periods.
430 (Supplementary Table 12).

431

432 First, we investigated if any Roman population contributed to the Byzantine or medieval groups, with
433 f_4 (norvegicus, Byzantine/medieval; Roman1, Roman2). We found that of two Roman geographical
434 groups (central European represented by Austria, and western Europe represented by Britain and the
435 Netherlands) the western rats were significantly more closely related to all the Byzantine and
436 medieval groups (Figure 4A, Supplementary Figure 10, Table 16). This result suggests that despite the
437 population turnover that occurred in temperate Europe after the Roman period, Roman black rats from
438 western Europe may have contributed to populations that colonized temperate Europe following the
439 decline of the original population.

440

441 Next, we applied f_4 (norvegicus, Roman; Byzantine/medieval1, Byzantine/medieval2) to test if there
442 were any differences in the relative contribution of Roman rat ancestry into the Byzantine or medieval
443 populations. In agreement with the phylogenetic and MDS analysis, most northern groups were
444 significantly more closely related to the Roman rat populations compared to the Byzantine or more
445 recent southern groups (SML, MDT, Ass). The lone exception to this pattern were two post-medieval
446 samples from Buda Castle (BUD001/4), which were equally related to the Roman groups and the
447 Assos (Ass) group that consists of two samples from Byzantine Turkey (Supplementary Table 17).
448 Among the northern groups, the medieval rats from Åland (Finland), the UK and the Netherlands, as
449 well as Byzantine rats from Serbia, were more closely related to the Roman rat populations than were
450 medieval rats from central Europe (represented by populations in Germany, Czech Republic and
451 Hungary). This suggests that the genetic contribution from putatively western European Roman rats,
452 was also greater in the local western European medieval rats.

453

454 We also investigated the relationship between the Buda Castle (Hungary) samples from different time
455 periods by contrasting them with the other medieval rats from temperate Europe (Figure 4A,
456 Supplementary Figure 10, Table 18). As revealed by the phylogenetic tree, both the German and
457 Czech rats shared more genetic affinity with the c.14th-15th century Buda Castle (BUD003) sample,
458 than with the 17th century or later specimens (BUD001/4). Having said that, BUD001/4 still showed
459 higher affinity to BUD003, when compared with all other populations. This evidence suggests a black
460 rat population transition in this region between the 14th/15th century and the late 17th century,
461 potentially related to the 16th-17th century Ottoman occupation of Buda (Hungary), while the local
462 medieval ancestry was still present in the later population.

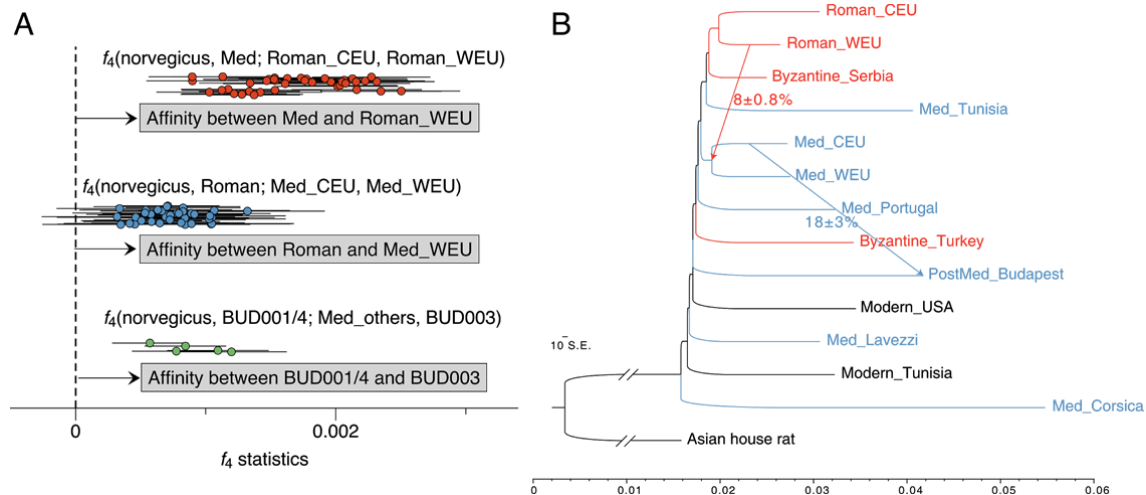
463

464 To corroborate the patterns of gene flow suggested by the f_4 -statistics, we used Treemix⁸⁴ to generate
465 an admixture graph of all ancient rat populations, using the Asian house rat as an outgroup. The
466 maximum-likelihood population tree without any admixture produced a similar topology to the
467 neighbor-joining autosomal phylogeny (Supplementary Figure 11). The rats from the northern group
468 and a medieval Tunisian rat formed a clade, to which all the other Mediterranean rats were an
469 outgroup, without any significant clustering pattern among the lineages. When admixture events were
470 allowed, the first two suggested gene flow edges were from the medieval central European population
471 into the post-medieval Buda Castle population, estimated to 18.2% +/- 3.0%, and from the Roman
472 western European population into the ancestral lineage of the medieval European populations in the
473 northern group, estimated to be 8.1% +/- 0.8% (Figure 4D).

474

475

476



477

478 **Figure 4. Gene flow among ancient rat populations.**

479 (A) The f -statistics showing admixture between different ancient rat populations. The dots show all
480 the combinations of f_4 -values as described above each cluster, and the error bars show $\pm 3SE$ of the
481 estimates. The three clusters show the affinity between: (top, red) medieval rats (Med) and western
482 European Roman rats (Roman_WEU);; (middle, blue) Roman rats (Roman) and western European
483 medieval rats (Med_WEU); and (bottom, green) post-medieval Buda Castle rats (BUD001/4) and the
484 medieval Buda Castle rat (BUD003), respectively.

485 (B) Admixture graph with two migration events fitted, estimated by Treemix. The migration edges are
486 displayed by arrow including the introgression fractions and standard errors. The color of each branch
487 represents the time period of each group: Roman/Byzantine (red) and medieval / post-medieval (blue).

488

489 The results from both the f -statistics and Treemix analyses revealed a degree of Roman rat ancestry in
490 the medieval populations. More specifically, medieval rats were more closely related to the Roman rat
491 populations from the Netherlands and Britain (Figure 4, Supplementary Table 16). This signal
492 suggests a reservoir of black rat population in western Europe that admixed with the re-introduced
493 medieval population. The stronger affinity of medieval western European populations to Roman
494 populations (Supplementary Table 17) also suggested that this relict population was more likely
495 distributed in western and not central Europe. This result could indicate that rats from the
496 northernmost Roman provinces were not extirpated, despite their absence in early medieval
497 zooarchaeological assemblages. Alternatively, and in our view more likely, the inferred relict
498 population may have been located in an unsampled region of France or southwest Europe. The
499 observation that medieval rats from temperate Europe fall into the same cluster as Roman rats also
500 suggests that the second (medieval) wave of introduction to temperate Europe probably originated
501 from the same source population as the first (Roman) dispersal. Considering the zooarchaeological
502 evidence that rat populations in southern Europe persisted after the collapse of the Western Roman
503 Empire, notably in Italy⁴⁰, it is likely that southern Europe was the source of reintroduced rats in
504 temperate Europe.

505

506 Given the presence of rats in 9th century northern *emporium* (proto-urban trading sites) around the North
507 and Baltic Seas^{46,49,50}, a southern European origin would emphasise the importance of the Carolingian
508 Empire (the Frankish polity which controlled much of western and central Europe as well as northern
509 Italy in the 9th century CE) and routes such as the Rhône and Rhine corridors in reestablishing large-
510 scale trade links between the Mediterranean and northern Europe⁸⁵. This connection remains tentative
511 until samples from the early emporia themselves in mainland Italy and the Iberian Peninsula can be
512 investigated. Samples from the early Islamic world derived from the Iberian Peninsula and North
513 Africa would also help to clarify the population history of black rats.

514

515 **Conclusion**

516 This study explores the historic dispersal of commensal black rats using a *de novo* genome assembly
517 for the black rat, ancient and modern mtDNA from across Europe, Africa, and the Indian Ocean, and
518 ancient nuclear genomes from the Mediterranean and Europe. Our results suggest that the black rat
519 was most likely introduced to the eastern Mediterranean by an overland route through Southwest
520 Asia, though a maritime route via the Indian Ocean and Red Sea cannot be excluded. We identify two
521 waves of rat introduction into temperate Europe. The first likely accompanied the Roman northward
522 expansion during the first centuries BCE/CE and the second took place during the medieval period
523 (starting in the 8th-10th centuries). The rats in this second wave were probably derived from the same
524 ancestral population as the first, and subsequently admixed with a western or southern European relict
525 population from the first wave.

526 Considered alongside the paucity of archaeological rat remains from the 6th-8th centuries CE
527 (particularly in northern and western Europe), this population turnover suggests that the black rat
528 population and range declined during the early medieval period. This may have been associated with
529 the breakdown of the Roman Empire - from the 5th century CE in western Europe and the early 7th
530 century CE in the Balkans - and with it, the network of well-connected settlements that had previously
531 supported black rat populations. Grain shipments may have played a key role in the dispersal and
532 maintenance of rat populations during the Roman period, and it is notable that weevils (*Sitophilus*
533 *granarius*) and other grain pests show a similar pattern of Roman introduction, apparent post-Roman
534 extirpation, and a medieval reintroduction in the northern provinces⁸⁶. Alternatively, or additionally,
535 European rat populations may have been negatively impacted by the First Plague Pandemic and/or the
536 climatic cooling of the Late Antique Little Ice Age, both of which began in the mid-6th century CE. To
537 disentangle these scenarios, further zooarchaeological and genomic studies of ancient rats are required
538 that span these centuries across a wider geographic range.

539 The medieval introduction of rats into Northern Europe is attested (at the latest) by their presence in
540 Germany in the early 10th century, coincident with an increase in rat bone finds across the continent.
541 Our results suggest a repopulation of temperate Europe from the south, perhaps linked with the
542 development of trade routes in Carolingian western Europe, and probably not via early Russian
543 riverine trade, as has been previously hypothesised³². Black rats appear to have been a continuous
544 presence in Europe from this point until the post-medieval period spanning the 14th century Black
545 Death and extending into the 17th century. This population may also have been supplemented by
546 localised introductions, including one potentially associated with the Ottoman occupation of Buda
547 from 1541 CE).

548 The near extirpation of black rats in modern Europe is likely linked to competition with the brown rat
549 which arrived from Asia in the early 18th century^{52,53}. The genetic and demographic impact of this
550 dispersal on black rats is an important area for future investigations since by the late 18th century,

551 naturalists in many European countries had already attributed a marked decline in *R. rattus* to
552 competition from *R. norvegicus*^{87–90}. The black rat’s significantly reduced, but persistent presence,
553 particularly in towns, suggests a degree of niche partitioning between the two species⁹¹.

554 Our results reveal the degree to which human-commensal species can undergo population dispersal
555 and demographic fluctuations. In fact, because these dynamic evolutionary processes are tightly
556 correlated with the characteristics of the human niche, commensal species can act as ideal proxies to
557 interpret the history of human movement and cultural change.

558

559 **Methods**

560 **Radiocarbon dating and calibration**

561 Fourteen ancient rat bones were radiocarbon dated via accelerator mass spectrometry (AMS) on bone
562 collagen at Manheim (MAMS), University of Waikato (Wk), and Oxford University (OxA), and these
563 were analysed alongside two previously published dates from Gatehampton⁹² (Supplementary Table
564 12). One additional sample (SNE002 / Wk-51521) failed due to insufficient collagen. All radiocarbon
565 dates were calibrated in OxCal 4.4⁹³, using the IntCal20 calibration curve⁹⁴.

566

567 Given the omnivorous diet of black rats, stable isotope values were monitored for evidence of marine
568 dietary contributions that might result in significant reservoir effects. Where possible, $\delta^{13}\text{C}$ (‰ vs.
569 VPDB) and $\delta^{15}\text{N}$ values (‰ vs. AIR) were obtained by the respective dating laboratories using
570 Isotope Ratio Mass Spectrometry (IRMS) and their standard protocols; otherwise $\delta^{13}\text{C}$ values were
571 used as reported from the AMS. Nitrogen isotope values were available for 10 specimens and fell
572 between 6.9‰-11.9‰, consistent with published data for commensal brown rats⁹⁵ and with an
573 omnivorous diet. Carbon isotope values ranged from -21.9‰ to -17.4‰. In the absence of detailed
574 local comparative isotope data from terrestrial and marine species, it was not possible confidently to
575 estimate marine dietary contribution and hence, the magnitude of any required correction.

576 Nonetheless, we performed indicative corrections for specimens whose $\delta^{13}\text{C}$ values suggested a
577 possible non-negligible marine component in order to test for any possible impact on our
578 interpretations. The cut-off for this was set as -18.5‰, based on published values for European
579 terrestrial herbivores and the enrichment expected due to trophic level in an omnivore.

580

581 For six specimens with $\delta^{13}\text{C} > -18.5$ ‰, percentage marine contribution was estimated using “formula
582 1” from⁹⁶, with terrestrial and marine endpoints of -21‰ and -12‰ respectively and a trophic
583 enrichment factor of 1‰. These values were used to recalibrate the dates using mixed IntCal20 and
584 Marine20⁹⁷ curves, and the magnitude of potential offset was assessed. In no cases did the median
585 calibrated date change by more than 140 years, and in no case would it have moved a specimen into a
586 different chronological category or altered our interpretations. Given the uncertainty inherent in this

587 process, the uncorrected ranges are used in Figure 3, and details of the indicative corrections are given
588 in Supplementary Table 12. In the majority of cases, the uncorrected date range coincided more
589 closely with the stratigraphic dating.

590

591 ***De novo* genome assembly**

592 The black rat genome was sequenced and assembled using DNA extracted from the liver of a male
593 wild-caught individual from California, USA. Shotgun, Chicago and Dovetail Hi-C libraries were
594 prepared and sequenced on Illumina HiSeq 4000 platform and the genome was assembled using
595 Meraculous⁹⁸ and HiRise scaffolding pipeline⁶⁴. The detailed information of genome assembly is
596 provided in the Supplementary Note 2.

597

598 The repetitive regions were identified using RepeatMasker 4.0.7⁹⁹ with Repbase 20170127 and the
599 query species set as *rattus*, and TRF 4.09 (Tandem repeats finder)¹⁰⁰, with parameters set as “2 7 7 80
600 10 50 12”. The completeness of genome assembly was assessed by BUSCO 3.0.2⁶⁵, using the 303
601 orthologs in Eukaryota odb9 dataset. The new genome assembly was aligned to the brown rat
602 reference genome *Rnor_6.0* using nucmer 4.0.0 in MUMmer tool package¹⁰¹, to investigate the
603 synteny between *R. rattus* and *R. norvegicus* genomes, using both masked assemblies and anchor
604 matches that are unique in both reference and query (Supplementary Note 2).

605

606 **Mitochondrial Cytochrome B fragment sequencing**

607 Overall, 292 tissue samples identified as *R. rattus* were included for analysis, including 263 museum
608 specimens (sampled from the collections at: American Museum of Natural History, British National
609 History Museum, Field Museum Chicago) and 29 modern specimens collected in the field
610 representing a wide geographic area at the periphery and on islands within the Indian Ocean.

611

612 DNA extraction and sequencing of these modern and museum samples were conducted in the modern
613 laboratory at the Archaeology Department of Durham University, following standard protocols
614 (Supplementary Note 4). The *cytb* region was amplified in 10 overlapping fragments and a variety of
615 primer combinations was used depending on the nature of the sample (Supplementary Table 19). The
616 sequencing reaction was carried out by the DNA Sequencing Service at the School of Biological and
617 Biomedical Sciences at Durham University. The sequencing chromatograms were edited manually,
618 subsequently assembled, and a consensus sequence per individual exported using Geneious R6
619 version 6.0.6¹⁰². Standard anti-contamination guidelines were followed. We successfully amplified
620 *cytb* sequences from 202 of 292 samples. Only those that possessed >90% gene coverage were
621 included in the analysis, which left 132 sequences.

622

623 **Ancient DNA extraction and processing**

624 We sampled 191 ancient black rats and eight modern black rat individuals from 33 archaeological
625 sites across Europe and three sites in North Africa (Supplementary Table 7, Note 1). Where multiple
626 samples were taken from the same or related archaeological contexts, care was taken to ensure that
627 these represented discrete individuals - either by sampling the same skeletal element and side, or on
628 the basis of differing size and / or age.

629

630 Ancient DNA extraction was performed in dedicated ancient DNA facilities at the University of
631 Oxford, the Max Planck Institute for the Science of Human History in Jena and the University of
632 York. All of the ancient lab facilities followed standard ancient DNA laboratory practices to minimise
633 contamination, including the use of blanks at each stage from extraction to amplification. All material
634 analysed at Oxford underwent the following treatment. Due to the small size of black rat bones, the
635 outer surface of the bones was not removed prior to extraction. Bones that weighed <50 mg were
636 completely consumed during the extraction process. The bone or tooth was cut using a Dremel drill
637 with a clean cutting wheel per sample (Dremel no 409) and pulverised in a Micro-dismembrator
638 (Sartorius-Stedim Biotech). Material analysed at York was subjected to bleach treatment (6%
639 sodium hypochlorite for 5 minutes, and then rinsed with ultrapure water 3 times) prior to powdering
640 following the same procedure as Oxford.

641

642 Extractions performed in Jena followed a silica-based protocol¹⁰³ using 50mg of bone powder.
643 Extractions performed at the University of Oxford were conducted using the Dabney protocol with a
644 modification of the addition of a 30 minute pre-digestion stage¹⁰⁴. Extractions performed at the
645 University of York were conducted using¹⁰⁵ as modified in¹⁰⁶.

646

647 For each sample processed in Jena, a double-stranded DNA sequencing library was prepared from 20
648 µL of extract, with partial uracil-DNA-glycosylase (UDG) treatment (hereafter denoted as
649 ds_halfUDG) or without UDG treatment (ds_nonUDG), following a published protocol¹⁰⁷. Sample-
650 specific index combinations were added to the sequencing libraries^{108,109}. The indexed libraries were
651 shotgun sequenced on an Illumina HiSeq 4000 instrument for screening, with 75 single-end-run
652 cycles for ds_halfUDG libraries and 75 double-end-run cycles for ds_nonUDG libraries. After
653 screening, one ds_nonUDG library and seven ds_halfUDG libraries were deep sequenced in the
654 University of Kiel, on an Illumina HiSeq 4000 platform with 75 double-end-run cycles using the
655 manufacturer's protocol.

656

657 All extracts generated at the University of Oxford and the University of York were built into Illumina
658 libraries using double stranded methods using the Blunt-End Single-Tube Illumina library building
659 (BEST) protocol as described previously¹¹⁰ at the University of Oxford (ds_nonUDG). An additional
660 barcode was added to the IS1_adapter.P5 adapter resulting in a double external indexed library. The

661 libraries were then amplified on an Applied Biosystems StepOnePlus Real-Time PCR system, to
662 determine both the success of the library build and the number of optimum cycles to use for the
663 indexing PCR reactions. These 164 libraries were pooled at equimolar concentrations ready for
664 sequencing. The pool of libraries was sequenced on an Illumina HiSeq 4000 (paired-end 75 bp) at the
665 Danish National High-Throughput Sequencing Centre for screening at Novogene, Sacramento.

666

667 Ten extracts from Oxford were built into single-stranded libraries at the Max Planck Institute for
668 Evolutionary Anthropology in Leipzig, Germany. The libraries were built from 30µl of DNA extract
669 in the absence of uracil DNA glycosylase (ss_nonUDG) followed by double indexing, using an
670 automated version of the protocols described in ^{108,109} on a liquid handling system (Agilent
671 Technologies Bravo NGS Workstation). From the initial screening run results 31 ds_nonUDG
672 libraries from Oxford were included for deeper sequencing in Jena, together with the ten ss_nonUDG
673 libraries, on an Illumina HiSeq 4000 platform with 75 single-end-run cycles (Supplementary Table
674 11).

675

676 **Genotyping and dataset preparation**

677 The shotgun sequencing reads from 39 ancient and modern black rats were cleaned and mapped to the
678 *de novo* *R. rattus* genome assembly using EAGER pipeline 1.92.55 ¹¹¹. Within the pipeline, the
679 adapters were removed by AdapterRemoval 2.2.0 ¹¹², reads were mapped with BWA 0.7.12 aln/samse
680 algorithm ¹¹³, duplications were removed by DeDup 0.12.1 (<https://github.com/apeltzer/DeDup>) and
681 damage patterns of each library were checked with mapDamage 2.0.6 ¹¹⁴. For the seven ds_halfUDG
682 libraries, we masked 2bp from both ends of the reads using trimBam in bamUtil 1.0.13 ¹¹⁵ to remove
683 the damaged sites.

684

685 The shotgun sequencing reads from four modern individuals, including the Californian black rat for
686 *de novo* genome assembly, two published *R. norvegicus* individuals (Accession: ERS215789,
687 ERS215791) ⁶⁷ and one published *R. tanezumi* individual (Accession: SRS1581480, HXM4) ¹¹⁶ were
688 mapped to the genome assembly using the BWA 0.7.12 mem algorithm. After using a mapping
689 quality filtering of 30 and removing reads with multiple hits, duplications were removed using
690 DeDup. We then performed indel realignment for cleaned bam files of both ancient and modern
691 individuals using RealignerTargetCreator and IndelRealigner in The Genome Analysis Toolkit
692 (GATK) v3.5-0 ¹¹⁷.

693

694 For the demographic history analysis, we called diploid genotypes from three modern genomes using
695 the highest coverage genome of each of the species: *R. rattus* (CP-5999), *R. norvegicus* (ERS215791)
696 and *R. tanezumi* (HXM4). Each of the bam files was piled up using samtools mpileup, using reads
697 with mapping quality and base quality over 30, and BAQ disabled. Bi-allelic SNPs were then

698 individually called using bcftools call -m mode and filtered for SNPs with phred-scaled quality score
699 (QUAL) over 30, sequence depth between 0.5-2X mean coverage, and not within 5bp of an indel.
700 After masking for repetitive regions, the consensus sequences of 18 largest autosomal scaffolds were
701 generated, with heterozygous sites represented by IUPAC nucleotide code.

702

703 The sequencing reads of ancient and modern black rats after AdapterRemoval were also mapped to *R.*
704 *rattus* reference mitochondrial sequence NC_012374.1 with BWA 0.7.12 aln/samse algorithm and
705 realigned with CircularMapper¹¹¹. The reads of *R. norvegicus* and *R. tanezumi* individuals were
706 mapped to mitochondrial references of *R. norvegicus* (NC_001665.2) and *R. tanezumi*
707 (NC_011638.1), respectively. After removing duplication using DeDup, the consensus sequences
708 were generated by Schmutzi with a quality threshold of 30¹¹⁸.

709

710 We called the pseudo-haploid genotypes in autosomal regions, from all modern and ancient
711 individuals using ANGSD 0.931¹¹⁹, with parameter “-doHaploCall 1” to randomly sample one base.
712 As the 18 longest autosomal scaffolds covered >99% of the autosomal assembly, we only called
713 genotypes on the non-repetitive regions of these 18 scaffolds. We applied “-remove_bads 1 -
714 uniqueOnly 1 -minMapQ 30 -minQ 30 -C 50 -baq 1” parameters to filter out reads that had multiple
715 hits, with mapping quality or base quality less than 30, perform base alignment quality (BAQ)
716 computation and adjust mapping quality based for excessive mismatches¹²⁰. To remove the
717 deamination-induced damages in ancient DNA molecules, we only kept the transversion variants for
718 downstream analysis. The genotypes on single-copied male-specific Y-chromosome regions
719 (scpMSY) were called from all male individuals using ANGSD 0.931, with the same filters as
720 autosomal genotyping, and -doHaploCall 2 to get the major call. The detailed information of scpMSY
721 regions identification was provided in Supplementary Note 2.

722

723 To estimate the heterozygosity rates of ancient rat samples, the cleaned reads with base quality and
724 mapping quality over 30 were piled up with mpileup in SAMtools 1.3¹²¹. We then called pseudo-
725 diploid genotypes with pileupCaller 1.2.2 (<https://github.com/stschiff/sequenceTools>) under random
726 diploid calling mode, which randomly sampled two reads at each site, on the transversion variants
727 identified in ANGSD. The heterozygosity rates calculated from pseudo-diploid genotypes were half of
728 the real heterozygosity rates of the samples on these variants.

729

730 **Demographic history analysis**

731 The population size dynamics was estimated using PSMC 0.6.5⁶⁶, with parameter “-N25 -t20 -r5 -p
732 “4+25*2+4+6”” and 100 bootstrap replicates. The PSMC output was visualized with generation time
733 of 0.5 years and mutation rate $\mu = 3 \times 10^{-9}$ site/generation, based on an estimate calculated in a previous
734 study of *R. norvegicus*⁶⁷.

735

736 G-PhoCS⁶⁸ was applied to estimate the population sizes, population divergence times and migration
737 rates among three rat species, using the three high-coverage diploid genomes. The analysis was
738 performed on 38,078 loci of 1kb length, identified in non-repetitive, autosomal regions. A preliminary
739 analysis with all possible migration events was first run for 250,000 generations, then two parallel
740 runs for 500,000 generations with one migration event were carried out for parameter estimation.
741 Finally, the estimated parameters were converted to effective population sizes (N_e), divergence times
742 (T) and total migration rates (m_{total}) as described in⁶⁸: $\theta = 4 * N_e * \mu$, $\tau = T * \mu / g$ and
743 $m_{total} = m * \tau$, with mutation rate $\mu = 2.96 * 10^{-9}$ site/generation and generation time (g) of 0.5 years.
744 The detailed information for loci selection and analysis was provided in Supplementary Note 3.

745

746 **Phylogenetic analysis**

747 The ancient mitochondrial genomes were analyzed alongside seven modern reference genomes,
748 including the modern Californian black rat from the reference genome assembly, two published *R.*
749 *norvegicus* individuals⁶⁷, one published *R. tanezumi* individual¹¹⁶ and the published mitochondrial
750 genome references of the three species (*R. rattus* NC_012374.1, *R. tanezumi* NC_011638.1, *R.*
751 *norvegicus* NC_001665.2). The haplotypes were aligned using MUSCLE v3.8.1551¹²² with default
752 parameters, and the best-fit model was selected based on Akaike Information Criterion (AIC)
753 calculated by jmodeltest v2.1.10¹²³. Then Maximum Likelihood (ML) tree was built using RAxML
754 v8.2.12¹²⁴, with GTR+I+G model and 100 bootstrap replicates.

755

756 The cytb region of the mitochondrial genome haplotypes were extracted using MEGA7, and
757 combined with modern cytb haplotypes from previous publications^{10,24,69,70} and this study. We aligned
758 the data using MAFFT v7.123b¹²⁵, then built a ML tree using RAxML v8.2.9¹²⁴, with GTR+I+G
759 model and 1000 bootstrap replicates.

760

761 The autosomal phylogeny was reconstructed using neighbor-joining (NJ) method implemented in
762 package Ape 5.3 in R 3.5.1. The distance matrix was calculated based on 3,393,710 autosomal
763 transversion variants, after removing singletons, using the genetic distance described in⁶⁸.
764 Bootstrapping was performed by resampling the variants from 100 kb non-overlapping windows, and
765 the support on each node was calculated based on 100 bootstrap replicates. The phylogenetic tree
766 based on Y-chromosome scpMSY regions was built with RaxML 8.2.12¹²⁴, using GTR substitution
767 model, ML estimation of base frequencies and 100 rapid bootstrapping replicates.

768

769 **Population genetics analysis**

770 The IBS distance matrix among individuals was calculated using PLINK v1.90b¹²⁶ with parameter "--
771 distance 1-ibs". MDS analysis was performed using PLINK and ten dimensions were calculated on

772 both datasets including all studied samples and *R. rattus* samples only. The f_4 -statistics were
773 calculated by *qpDstat* 755 in ADMIXTOOLS 5.1 package ¹²⁷, with parameter “f4 mode: YES”, and
774 the two *R. norvegicus* individuals were used as outgroup in all the analysis.

775

776 We also applied Treemix 1.13 ⁸⁴ to simultaneously infer the population structure and admixture events
777 among black rat populations. The black rat samples were grouped based on the geographic location,
778 time period and phylogenetic pattern identified in previous analysis (Supplementary Table 11). The
779 allele frequency was calculated by PLINK and 1,145,713 sites covered in at least one sample from
780 each group were included in the analysis. We built the admixture graph assuming 0 to 10 migration
781 events, with parameters “-k 500 -global -se -noss -root tanezumi” to group 500 SNPs per block for
782 covariance matrix estimation. We then performed a global rearrangement after adding all the
783 populations, calculated standard errors of migration weights, disabled sample size correction and
784 assigned *R. tanezumi* as the root of the topology.

785

786 **Data availability**

787 The *R. rattus* genome assembly is available in the NCBI under the accession number
788 GCA_011800105.1. Aligned reads from the 39 newly reported ancient black rats are available at the
789 ENA archive under the accession number ([provided upon acceptance](#)). The mitochondrial genome
790 haplotypes are available under the accession number ([provided upon acceptance](#)).

791

792 **Acknowledgements**

793 We thank the wet laboratory teams at MPI-SHH, the PalaeoBARN at the University of Oxford and the
794 University of York. We thank David K. James and Lucia Hui of the Alameda County Vector Control
795 Services District for procuring the rat used for the *de novo* genome. We are grateful to Sarah Nagel at
796 Max Planck Institute for the Evolutionary Anthropology for the single-stranded library preparation,
797 and Dovetail Genomics for the *de novo* genome assembly service. We thank Maria Spyrou for her
798 suggestions and comments. We acknowledge Ewan Chipping and Helena England (University of
799 York), Carl Phillips, Veronica Lindholm (Ålands Museum), Christine McDonnell and Nienke van
800 Doorn (York Archaeological Trust), Emile Mittendorf (Gemeente Deventer), Inge Riemersma
801 (Archaeological depot, Provincie Zuid-Holland), the Turkish Ministry of Culture & Tourism, Jan
802 Frolík and Iva Herichová (Institute of Archaeology of the Czech Academy of Sciences, Prague),
803 Franz Humer and Eduard Pollhammer (Archaeological Park Carnuntum), Dorottya B. Nyékhelyi and
804 László Daróczi-Szabó (Budapest History Museum), Institut National du Patrimoine (Tunisia),
805 University of Barcelona, Spanish Ministry of Science and Innovation (Project HUM2006-
806 03432/HIST), Spanish Ministry of Culture (program of archaeological excavations abroad 2009);
807 Spanish Agency of International Cooperation for the Development (2009), Catalan Institute of
808 Classical Archaeology (ICAC), Vujadin Ivanisević, Nemanja Marković and Ivan Bugarski

809 (Archaeological Institute Belgrade), the Field Museum Chicago, the British National History Museum
810 and the American Museum of Natural History for providing materials and support. G.L. and A.J. were
811 supported by the ERC (grant ERC-2013-StG-337574-UNDEAD) and A.J. was supported by the
812 Natural Environment Research Council Doctoral Training Program. D.O. was supported by Wellcome
813 (Small Grant in Humanities and Social Science 209817/Z) and the British Academy / Leverhulme
814 Trust (Small Research Grant SG170938). E.R. was supported by Estonian Research Council grant No
815 PRG29. R.K. was supported by the Czech Academy of Sciences institutional support
816 (RVO:67985912). S.V.-L. was supported by the ERC (grant ERC-StG- 716298 ZooMWest). H.E. was
817 funded by an ERC grant (206148) through the Sealinks Project. A.H.B was funded by the Leverhulme
818 Trust (ECF-2017-315). The *de novo* genome assembly, population genomics study, and radiocarbon
819 dating were funded by the Max Planck Society.

820

821 **Author contributions**

822 J.K., G.L. and D.O. designed the project; A.J., B.K.-K., B.K., C.S., H.A.-J., H.E., A.T. generated data;
823 H.Y., A.J. and D.O. analyzed data; G.A, N.B., H.B., B.B.-A., W.B., A.C., C.J.C., T.C., K.D., K.E.,
824 J.F., L.G., E.G., P.G., S.G., S.H.-D., C.H., R.H., N.K., H.K., Z.K., K.K., R.K., A.L., B.M.-T., A.M.-
825 M., M.N., T.O°C., T.Ou, E.Q.M., K.P., J.P., N.P., S.R., J.R., E.R., J.S., J.S.G., E.T., S.V.-L., I.van der
826 J., W.V.N., J.-D.V., T.W., S.W.-J. and J.Z. provided material and support; H.Y., D.O., A.J., A.H.-B.,
827 G.L. and J.K. wrote the paper with contributions from all other authors.

828

829 **References**

- 830 1. Boivin, N. L. *et al.* Ecological consequences of human niche construction: Examining long-term
831 anthropogenic shaping of global species distributions. *Proc. Natl. Acad. Sci. U. S. A.* **113**, 6388–
832 6396 (2016).
- 833 2. Capizzi, D., Bertolino, S. & Mortelliti, A. Rating the rat: global patterns and research priorities in
834 impacts and management of rodent pests. *Mamm. Rev.* **44**, 148–162 (2014).
- 835 3. Meerburg, B. G., Singleton, G. R. & Kijlstra, A. Rodent-borne diseases and their risks for public
836 health. *Crit. Rev. Microbiol.* **35**, 221–270 (2009).
- 837 4. McCormick, M. Rats, Communications, and Plague: Toward an Ecological History. *J.*
838 *Interdiscip. Hist.* **34**, 1–25 (2003).
- 839 5. Aplin, K. P., Brown, P., Jacob, J., Krebs, C. J. & Singleton, G. R. *Field methods for rodent*
840 *studies in Asia and the Indo-Pacific.* (2003).

- 841 6. Lack, J. B. *et al.* Invasion facilitates hybridization with introgression in the *Rattus rattus* species
842 complex. *Mol. Ecol.* **21**, 3545–3561 (2012).
- 843 7. Conroy, C. J. *et al.* Cryptic genetic diversity in *Rattus* of the San Francisco Bay region,
844 California. *Biol. Invasions* **15**, 741–758 (2013).
- 845 8. Robins, J. H., Hingston, M., Matisoo-Smith, E. & Ross, H. A. Identifying *Rattus* species using
846 mitochondrial DNA. *Mol. Ecol. Notes* **7**, 717–729 (2007).
- 847 9. Pagès, M. *et al.* Revisiting the taxonomy of the Rattini tribe: a phylogeny-based delimitation of
848 species boundaries. *BMC Evol. Biol.* **10**, 184 (2010).
- 849 10. Aplin, K. P. *et al.* Multiple geographic origins of commensalism and complex dispersal history
850 of Black Rats. *PLoS ONE* **6**, e26357 (2011).
- 851 11. Robins, J. H. *et al.* Dating of divergences within the *Rattus* genus phylogeny using whole
852 mitochondrial genomes. *Mol. Phylogenet. Evol.* **49**, 460–466 (2008).
- 853 12. Yosida, T. H., Kato, H., Tsuchiya, K. & Moriwaki, K. Karyotypes and serum transferrin patterns
854 of hybrids between Asian and Oceanian black rats, *Rattus rattus*. *Chromosoma* **34**, 40–50 (1971).
- 855 13. Hulme-Beaman, A., Dobney, K., Cucchi, T. & Searle, J. B. An Ecological and Evolutionary
856 Framework for Commensalism in Anthropogenic Environments. *Trends Ecol. Evol.* **31**, 633–645
857 (2016).
- 858 14. Jones, E. P., Eager, H. M., Gabriel, S. I., Jóhannesdóttir, F. & Searle, J. B. Genetic tracking of
859 mice and other bioproxies to infer human history. *Trends Genet.* **29**, 298–308 (2013).
- 860 15. Puckett, E. E., Orton, D. & Munshi-South, J. Commensal Rats and Humans: Integrating Rodent
861 Phylogeography and Zooarchaeology to Highlight Connections between Human Societies.
862 *Bioessays* e1900160 (2020).
- 863 16. Jones, E. P. *et al.* Fellow travellers: a concordance of colonization patterns between mice and
864 men in the North Atlantic region. *BMC Evol. Biol.* **12**, 35 (2012).
- 865 17. Cucchi, T. Uluburun shipwreck stowaway house mouse: molar shape analysis and indirect clues
866 about the vessel's last journey. *J. Archaeol. Sci.* **35**, 2953–2959 (2008).
- 867 18. Cucchi, T. *et al.* On the trail of Neolithic mice and men towards Transcaucasia:
868 zooarchaeological clues from Nakhchivan (Azerbaijan). *Biol. J. Linn. Soc. Lond.* **108**, 917–928

- 869 (2013).
- 870 19. Cucchi, T. *et al.* Tracking the Near Eastern origins and European dispersal of the western house
871 mouse. *Sci. Rep.* **10**, 8276 (2020).
- 872 20. Matisoo-Smith, E. & Robins, J. H. Origins and dispersals of Pacific peoples: evidence from
873 mtDNA phylogenies of the Pacific rat. *Proc. Natl. Acad. Sci. U. S. A.* **101**, 9167–9172 (2004).
- 874 21. Matisoo-Smith, E. & Robins, J. Mitochondrial DNA evidence for the spread of Pacific rats
875 through Oceania. *Biol. Invasions* **11**, 1521–1527 (2009).
- 876 22. West, K. *et al.* The Pacific Rat Race to Easter Island: Tracking the Prehistoric Dispersal of
877 *Rattus exulans* Using Ancient Mitochondrial Genomes. *Frontiers in Ecology and Evolution* **5**, 52
878 (2017).
- 879 23. Niethammer, V. J. Zur Taxonomie und Ausbreitungsgeschichte der Hausratte (*Rattus rattus*).
880 *Zool. Anz. Jena* **194**, 405–415 (1975).
- 881 24. Baig, M., Khan, S., Eager, H., Atkulwar, A. & Searle, J. B. Phylogeography of the black rat
882 *Rattus rattus* in India and the implications for its dispersal history in Eurasia. *Biol. Invasions* **21**,
883 417–433 (2019).
- 884 25. Tchernov, E. Commensal animals and human sedentism in the Middle East. *Animals and*
885 *archaeology* **3**, 91–115 (1984).
- 886 26. Ervynck, A. Sedentism or urbanism? On the origin of the commensal black rat (*Rattus rattus*). in
887 *Bones and the Man: studies in honour of Don Brothwell* (eds. Dobney, K. & O'Connor, T. P.)
888 95–109 (Oxbow, 2002).
- 889 27. Ruffino, L. & Vidal, E. Early colonization of Mediterranean islands by *Rattus rattus*: a review of
890 zooarcheological data. *Biol. Invasions* **12**, 2389–2394 (2010).
- 891 28. Vigne, J.-D. & Valladas, H. È. Small Mammal Fossil Assemblages as Indicators of
892 Environmental Change in Northern Corsica during the Last 2500 Years. *J. Archaeol. Sci.* **23**,
893 199–215 (1996).
- 894 29. Oueslati, T. *et al.* ‘1st century BCE occurrence of chicken, house mouse and black rat in
895 Morocco: Socio-economic changes around the reign of Juba II on the site of Rirha’. *Journal of*
896 *Archaeological Science: Reports* **29**, 102162 (2020).

- 897 30. Audoin-Rouzeau, F. & Vigne, J.-D. La colonisation de l'Europe par le rat noir (*Rattus rattus*).
898 *Revue de Paléobiologie* **13**, 125–145 (1994).
- 899 31. Audoin-Rouzeau, F. & Vigne, et J.-D. Le rat noir (*Rattus rattus*) en Europe Antique et
900 médiévale: les voies du commerce et l'expansion de la peste. *Anthropozoologica* **25/26**, 399–404
901 (1997).
- 902 32. Armitage, P. L. Unwelcome companions: ancient rats reviewed. *Antiquity* **68**, 231–240 (1994).
- 903 33. Hufthammer, A. K. & Walløe, L. Rats cannot have been intermediate hosts for *Yersinia pestis*
904 during medieval plague epidemics in Northern Europe. *J. Archaeol. Sci.* **40**, 1752–1759 (2013).
- 905 34. Dean, K. R. *et al.* Human ectoparasites and the spread of plague in Europe during the Second
906 Pandemic. *Proc. Natl. Acad. Sci. U. S. A.* **115**, 1304–1309 (2018).
- 907 35. Sloane, B. *The Black Death in London*. (The History Press, 2011).
- 908 36. Hardy, A. The Under-Appreciated Rodent: Harbingers of Plague From the Middle Ages to the
909 Twenty-First Century. *J. Interdiscip. Hist.* **50**, 171–185 (2019).
- 910 37. White, L. A. & Mordechai, L. Modeling the Justinianic Plague: Comparing hypothesized
911 transmission routes. *PLoS One* **15**, e0231256 (2020).
- 912 38. O'Connor, T. P. On the lack of bones of the ship rat *Rattus rattus* from Dark Age York. *J. Zool.*
913 **224**, 318–320 (1991).
- 914 39. Rielly, K. The black rat. in *Extinctions and invasions: a social history of British fauna* (eds.
915 O'Connor, T. & Sykes, N.) 134–145 (Oxbow, 2010).
- 916 40. Salvadori, F. The transition from late antiquity to early Middle Ages in Italy. A
917 zooarchaeological perspective. *Quat. Int.* (2018) doi:10.1016/j.quaint.2018.06.040.
- 918 41. De Cupere, B. *et al.* Eagle owl (*Bubo bubo*) pellets from Roman Sagalassos (SW Turkey):
919 distinguishing the prey remains from nest and roost sites. *Int. J. Osteoarchaeol.* **19**, 1–22 (2009).
- 920 42. Parfitt, S. A. The small mammals. in *The transition to late antiquity on the Danube and beyond*
921 (ed. Poulter, A. G.) 198–318 (Oxford University Press, 2007).
- 922 43. Davis, E. M. Paleoecological studies at Stobi. in *Studies in the antiquities of Stobi* (eds.
923 Aleksova, B., Wiseman, J. & Mano-Zisi, Đ.) vol. 3 (Princeton University Press, 1981).
- 924 44. Baron, H., Reuter, A. E. & Marković, N. Rethinking ruralization in terms of resilience:

- 925 Subsistence strategies in sixth-century Caričin Grad in the light of plant and animal bone finds.
926 *Quat. Int.* **499**, 112–128 (2019).
- 927 45. Benedictow, O. J. *What Disease was Plague?: On the Controversy Over the Microbiological*
928 *Identity of Plague Epidemics of the Past*. (Brill, 2010).
- 929 46. O’Connor, T. P. *Bones from Anglo-Scandinavian levels at 16-22 Coppergate*. (Council for
930 British Archaeology, 1989).
- 931 47. Pasda, K. *Tierknochen als Spiegel sozialer Verhältnisse im 8.-15. Jh. in Bayern*.
932 (Praehistoricaverlag, 2004).
- 933 48. Dobney, K., Jacques, D., Barrett, J. & Johnstone, C. *Farmers, Monks and Aristocrats: the*
934 *environmental archaeology of Anglo-Saxon Flixborough*. (Oxbow, 2007).
- 935 49. Reichstein, H. *Die wildlebenden Säugetiere von Haithabu: Ausgrabungen 1966-1969 und 1979-*
936 *1980*. (Karl Wachholtz, 1991).
- 937 50. Wigh, B. *Animal husbandry in the Viking Age town of Birka and its hinterland: excavations in*
938 *the black earth 1990-95*. (Riksantikvarieämbetet, 2001).
- 939 51. Tourunen, A. *Animals in an Urban Context - A Zooarchaeological study of the Medieval and*
940 *Post-Medieval town of Turku*. (University of Turku, 2008).
- 941 52. Eryvnyck, A. *Archeozoölogisch onderzoek van de zwarte rat (Rattus rattus) en de bruine rat*
942 *(Rattus norvegicus)*. (Amsterdam, 1989).
- 943 53. Barrett-Hamilton, G. & Hinton, M. *A history of British mammals*. (Gurney and Jackson, 1910).
- 944 54. Mitchell-Jones, A. J. *The atlas of European mammals*. (Academic, 1999).
- 945 55. Savinetsky, A. B. & Krylovich, O. A. On the history of the spread of the black rat (*Rattus rattus*
946 *L.*, 1758) in northwestern Russia. *Biol. Bull. Russ. Acad. Sci.* **38**, 203–207 (2011).
- 947 56. Ward-Perkins, B. *The Fall of Rome and the End of Civilization*. (Oxford University Press, 2005).
- 948 57. Wickham, C. *Framing the Early Middle Ages: Europe and the Mediterranean, 400-800*. (Oxford
949 University Press, 2005).
- 950 58. Horden, P. & Purcell, N. *The Corrupting Sea: A Study of Mediterranean History*. (Wiley-
951 Blackwell, 2000).
- 952 59. Ambrosiani, B. Osten und Westen im Ostseehandel zur Wikingerzeit. in *Haithabu und die frühe*

- 953 *Stadtentwicklung im nördlichen Europa*. (eds. Brandt, K., Müller-Wille, M. & Radtke, C.) 339–
954 348 (Wachholtz, 2002).
- 955 60. Hodges, R. *Dark Age Economics: A New Audit*. (Bloomsbury, 2012).
- 956 61. Keller, M. *et al.* Ancient *Yersinia pestis* genomes from across Western Europe reveal early
957 diversification during the First Pandemic (541–750). *Proceedings of the National Academy of*
958 *Sciences* vol. 116 12363–12372 (2019).
- 959 62. Wagner, D. M. *et al.* *Yersinia pestis* and the Plague of Justinian 541–543 AD: a genomic
960 analysis. *The Lancet Infectious Diseases* vol. 14 319–326 (2014).
- 961 63. Feldman, M. *et al.* A High-Coverage *Yersinia pestis* Genome from a Sixth-Century Justinianic
962 Plague Victim. *Mol. Biol. Evol.* **33**, 2911–2923 (2016).
- 963 64. Putnam, N. H. *et al.* Chromosome-scale shotgun assembly using an in vitro method for long-
964 range linkage. *Genome Research* vol. 26 342–350 (2016).
- 965 65. Simão, F. A., Waterhouse, R. M., Ioannidis, P., Kriventseva, E. V. & Zdobnov, E. M. BUSCO:
966 assessing genome assembly and annotation completeness with single-copy orthologs.
967 *Bioinformatics* vol. 31 3210–3212 (2015).
- 968 66. Li, H. & Durbin, R. Inference of human population history from individual whole-genome
969 sequences. *Nature* **475**, 493–496 (2011).
- 970 67. Deinum, E. E. *et al.* Recent Evolution in *Rattus norvegicus* Is Shaped by Declining Effective
971 Population Size. *Mol. Biol. Evol.* **32**, 2547–2558 (2015).
- 972 68. Gronau, I., Hubisz, M. J., Gulko, B., Danko, C. G. & Siepel, A. Bayesian inference of ancient
973 human demography from individual genome sequences. *Nat. Genet.* **43**, 1031–1034 (2011).
- 974 69. Colangelo, P. *et al.* Mitochondrial phylogeography of the black rat supports a single invasion of
975 the western Mediterranean basin. *Biological Invasions* vol. 17 1859–1868 (2015).
- 976 70. Etougbétché, J. *et al.* Genetic diversity and origins of invasive black rats (*Rattus rattus*) in Benin,
977 West Africa. *fozo.1* **69**, 20014.1 (2020).
- 978 71. Hemamali, P. P. C. & Boyagoda, S. H. Historic black rat invasions into Sri Lanka lead to
979 hybridization forming two sub-lineages in the *Rattus rattus* species complex. *Ceylon Journal of*
980 *Science* vol. 49 433 (2020).

- 981 72. Carleton, G. G., Musserand, M. D. & Musser, G. G. Superfamily Muroidea. in *Mammal species*
982 *of the world: a taxonomic and geographic reference (3rd ed)*. (eds. Wilson, D. E. & Reeder, D.
983 M.) 894–1531 (Johns Hopkins University Press, 2005).
- 984 73. Boivin, N. Proto-globalisation and biotic exchange in the old world. in *Human dispersal and*
985 *species movement from prehistory to the present* (eds. Boivin, N., Crassard, R. & Petraglia, M.)
986 349–408 (Cambridge University Press, 2017).
- 987 74. Cooper, J. P. Egypt’s Nile-Red Sea canals: chronology, location, seasonality and function. in *Red*
988 *Sea IV: Connected Hinterlands* (eds. Blue, L., Cooper, J., Thomas, R. & Whitewright, J.) 195–
989 210 (Archaeopress, 2009).
- 990 75. Prendergast, M. E. *et al.* Reconstructing Asian faunal introductions to eastern Africa from multi-
991 proxy biomolecular and archaeological datasets. *PLoS One* **12**, e0182565 (2017).
- 992 76. Tollenaere, C. *et al.* Phylogeography of the introduced species *Rattus rattus* in the western Indian
993 Ocean, with special emphasis on the colonization history of Madagascar. *J. Biogeogr.* **37**, 398–
994 410 (2010).
- 995 77. Cobb, M. The Chronology of Roman Trade in the Indian Ocean from Augustus to Early Third
996 Century ce. *J. Econ. Soc. Hist. Orient* **58**, 362–418 (2015).
- 997 78. Ewer, R. F. The biology and behaviour of a free-living population of black rats (*Rattus rattus*).
998 *Animal Behaviour Monographs* **4**, 127–174 (1971).
- 999 79. Pocock, M. J. O., Hauffe, H. C. & Searle, J. B. Dispersal in house mice. *Biol. J. Linn. Soc. Lond.*
1000 **84**, 565–583 (2005).
- 1001 80. Büntgen, U. *et al.* Cooling and societal change during the Late Antique Little Ice Age from 536
1002 to around 660 AD. *Nat. Geosci.* **9**, 231–236 (2016).
- 1003 81. Perry, R. D. & Fetherston, J. D. *Yersinia pestis*--etiologic agent of plague. *Clin. Microbiol. Rev.*
1004 **10**, 35–66 (1997).
- 1005 82. Spyrou, M. A., Bos, K. I., Herbig, A. & Krause, J. Ancient pathogen genomics as an emerging
1006 tool for infectious disease research. *Nat. Rev. Genet.* **20**, 323–340 (2019).
- 1007 83. Fenwick, C. From Africa to Ifrīqiya: Settlement and Society in Early Medieval North Africa
1008 (650–800). *Al-Masāq* **25**, 9–33 (2013).

- 1009 84. Pickrell, J. K. & Pritchard, J. K. Inference of population splits and mixtures from genome-wide
1010 allele frequency data. *PLoS Genet.* **8**, e1002967 (2012).
- 1011 85. McCormick, M. Where do trading towns come from? Early medieval Venice and the northern
1012 emporia. *Post-Roman towns, trade and settlement in Europe and Byzantium* **1**, 41–68 (2007).
- 1013 86. Smith, D. & Kenward, H. Roman Grain Pests in Britain: Implications for Grain Supply and
1014 Agricultural Production. *Britannia* **42**, 243–262 (2011).
- 1015 87. Buffon, G.-L. L. C. de. *Histoire Naturelle, Générale et Particulière, avec la Description du*
1016 *Cabinet du Roi*. vol. 8 (L’Imprimerie Royale, 1760).
- 1017 88. Smith, R. *The Universal Directory for Taking Alive and Destroying Rats, and All Other Kinds of*
1018 *Four-footed and Winged Vermin, In a Method Hitherto Unattempted: Calculated for the Use of*
1019 *the Gentleman, the Farmer, and the Warrener*. (J. Walker, 1768).
- 1020 89. Pennant, T. *British Zoology*. (William Eyres, 1776).
- 1021 90. Rutty, J. *An essay towards a natural history of the County of Dublin*. vol. 1 (W. Sleater, 1772).
- 1022 91. O’Connor, T. Commensal Species. in *The Oxford Handbook of Animal Studies* (ed. Kalof, L.)
1023 (Oxford University Press, 2017).
- 1024 92. Walker, T., Sharpe, J. R. & Williams, H. Barn Owls and Black Rats from a Rural Roman Villa at
1025 Gatehampton, South Oxfordshire. *Environ. Archaeol.* 1–10 (2019).
- 1026 93. Bronk Ramsey, C. *OxCal*. (2020).
- 1027 94. Reimer, P. J., Austin, W. E. N., Bard, E. & Bayliss, A. The IntCal20 northern hemisphere
1028 radiocarbon age calibration curve (0–55 cal kBP). (2020).
- 1029 95. Guiry, E. & Buckley, M. Urban rats have less variable, higher protein diets. *Proc. R. Soc. B* **285**,
1030 20181441 (2018).
- 1031 96. Dewar, G. & Pfeiffer, S. Approaches to Estimating Marine Protein in Human Collagen for
1032 Radiocarbon Date Calibration. *Radiocarbon* **52**, 1611–1625 (2010).
- 1033 97. Heaton, T. J. *et al.* Marine20—The Marine Radiocarbon Age Calibration Curve (0–55,000 cal
1034 BP). *Radiocarbon* **62**, 779–820 (2020).
- 1035 98. Chapman, J. A. *et al.* Meraculous: de novo genome assembly with short paired-end reads. *PLoS*
1036 *One* **6**, e23501 (2011).

- 1037 99. Smit, AFA, Hubley, R & Green, P. RepeatMasker Open-4.0. <http://www.repeatmasker.org>
1038 (2013-2015).
- 1039 100. Benson, G. Tandem repeats finder: a program to analyze DNA sequences. *Nucleic Acids*
1040 *Research* vol. 27 573–580 (1999).
- 1041 101. Kurtz, S. *et al.* Versatile and open software for comparing large genomes. *Genome Biol.* **5**, R12
1042 (2004).
- 1043 102. Drummond, A. J. *et al.* Geneious v6. 1.6. (2011).
- 1044 103. Dabney, J. *et al.* Complete mitochondrial genome sequence of a Middle Pleistocene cave bear
1045 reconstructed from ultrashort DNA fragments. *Proceedings of the National Academy of Sciences*
1046 vol. 110 15758–15763 (2013).
- 1047 104. Damgaard, P. B. *et al.* Improving access to endogenous DNA in ancient bones and teeth. *Sci.*
1048 *Rep.* **5**, 11184 (2015).
- 1049 105. Yang, D. Y., Eng, B., Wayne, J. S., Dudar, J. C. & Saunders, S. R. Technical note: improved
1050 DNA extraction from ancient bones using silica-based spin columns. *Am. J. Phys. Anthropol.*
1051 **105**, 539–543 (1998).
- 1052 106. Speller, C. F. *et al.* Ancient mitochondrial DNA analysis reveals complexity of indigenous North
1053 American turkey domestication. *Proc. Natl. Acad. Sci. U. S. A.* **107**, 2807–2812 (2010).
- 1054 107. Rohland, N., Harney, E., Mallick, S., Nordenfelt, S. & Reich, D. Partial uracil–DNA–glycosylase
1055 treatment for screening of ancient DNA. *Philos. Trans. R. Soc. Lond. B Biol. Sci.* **370**, 20130624
1056 (2015).
- 1057 108. Gansauge, M.-T., Aximu-Petri, A., Nagel, S. & Meyer, M. Manual and automated preparation of
1058 single-stranded DNA libraries for the sequencing of DNA from ancient biological remains and
1059 other sources of highly degraded DNA. *Nat. Protoc.* (2020) doi:10.1038/s41596-020-0338-0.
- 1060 109. Kircher, M., Sawyer, S. & Meyer, M. Double indexing overcomes inaccuracies in multiplex
1061 sequencing on the Illumina platform. *Nucleic Acids Res.* **40**, e3 (2012).
- 1062 110. Carøe, C. *et al.* Single-tube library preparation for degraded DNA. *Methods Ecol. Evol.* **9**, 410–
1063 419 (2018).
- 1064 111. Peltzer, A. *et al.* EAGER: efficient ancient genome reconstruction. *Genome Biol.* **17**, 60 (2016).

- 1065 112. Schubert, M., Lindgreen, S. & Orlando, L. AdapterRemoval v2: rapid adapter trimming,
1066 identification, and read merging. *BMC Res. Notes* **9**, 88 (2016).
- 1067 113. Li, H. & Durbin, R. Fast and accurate short read alignment with Burrows-Wheeler transform.
1068 *Bioinformatics* **25**, 1754–1760 (2009).
- 1069 114. Jónsson, H., Ginolhac, A., Schubert, M., Johnson, P. L. F. & Orlando, L. mapDamage2.0: fast
1070 approximate Bayesian estimates of ancient DNA damage parameters. *Bioinformatics* **29**, 1682–
1071 1684 (2013).
- 1072 115. Jun, G., Wing, M. K., Abecasis, G. R. & Kang, H. M. An efficient and scalable analysis
1073 framework for variant extraction and refinement from population-scale DNA sequence data.
1074 *Genome Res.* **25**, 918–925 (2015).
- 1075 116. Teng, H. *et al.* Population Genomics Reveals Speciation and Introgression between Brown
1076 Norway Rats and Their Sibling Species. *Mol. Biol. Evol.* **34**, 2214–2228 (2017).
- 1077 117. McKenna, A. *et al.* The Genome Analysis Toolkit: a MapReduce framework for analyzing next-
1078 generation DNA sequencing data. *Genome Res.* **20**, 1297–1303 (2010).
- 1079 118. Renaud, G., Slon, V., Duggan, A. T. & Kelso, J. Schmutzi: estimation of contamination and
1080 endogenous mitochondrial consensus calling for ancient DNA. *Genome Biol.* **16**, 224 (2015).
- 1081 119. Korneliussen, T. S., Albrechtsen, A. & Nielsen, R. ANGSD: Analysis of Next Generation
1082 Sequencing Data. *BMC Bioinformatics* **15**, 356 (2014).
- 1083 120. Li, H. Improving SNP discovery by base alignment quality. *Bioinformatics* **27**, 1157–1158
1084 (2011).
- 1085 121. Li, H. *et al.* The Sequence Alignment/Map format and SAMtools. *Bioinformatics* **25**, 2078–2079
1086 (2009).
- 1087 122. Edgar, R. C. MUSCLE: multiple sequence alignment with high accuracy and high throughput.
1088 *Nucleic Acids Res.* **32**, 1792–1797 (2004).
- 1089 123. Darriba, D., Taboada, G. L., Doallo, R. & Posada, D. jModelTest 2: more models, new heuristics
1090 and parallel computing. *Nat. Methods* **9**, 772 (2012).
- 1091 124. Stamatakis, A. RAxML version 8: a tool for phylogenetic analysis and post-analysis of large
1092 phylogenies. *Bioinformatics* **30**, 1312–1313 (2014).

- 1093 125. Katoh, K. & Standley, D. M. MAFFT multiple sequence alignment software version 7:
1094 improvements in performance and usability. *Mol. Biol. Evol.* **30**, 772–780 (2013).
- 1095 126. Purcell, S. *et al.* PLINK: a tool set for whole-genome association and population-based linkage
1096 analyses. *Am. J. Hum. Genet.* **81**, 559–575 (2007).
- 1097 127. Patterson, N. *et al.* Ancient Admixture in Human History. *Genetics* vol. 192 1065–1093 (2012).
- 1098